


# Phosphorylation of STAT1 serine 727 enhances platinum resistance in uterine serous carcinoma

Xiang Zeng<sup>1</sup>, Tsukasa Baba <sup>1,2</sup>, Junzo Hamanishi<sup>1</sup>, Noriomi Matsumura<sup>3</sup>, Budiman Kharma<sup>1</sup>, Yuka Mise<sup>1</sup>, Kaoru Abiko<sup>1</sup>, Ken Yamaguchi<sup>1</sup>, Naoki Horikawa<sup>1</sup>, David G. Hunstman<sup>4,5</sup>, Kumuluzi Mulati<sup>1</sup>, Sachiko Kitamura<sup>1</sup>, Mana Taki<sup>1</sup>, Ryusuke Murakami<sup>1</sup>, Yuko Hosoe<sup>1</sup> and Masaki Mandai<sup>1</sup>

<sup>1</sup>Department of Gynecology and Obstetrics, Kyoto University Graduate School of Medicine, Kyoto, Japan

<sup>2</sup>Department of Obstetrics and Gynecology, Iwate Medical University School of Medicine, Iwate, Japan

<sup>3</sup>Department of Obstetrics and Gynecology, Kindai University Faculty of Medicine, Osaka, Japan

<sup>4</sup>Department of Pathology and Laboratory Medicine, University of British Columbia, British Columbia Cancer Agency, Vancouver, BC, Canada

<sup>5</sup>Genetic Pathology Evaluation Centre, Vancouver General Hospital, Vancouver, BC, Canada

Uterine serous carcinoma (USC) is a highly aggressive histological subtype of endometrial cancers harboring highly metastatic and chemoresistant features. Our previous study showed that STAT1 is highly expressed in USC and acts as a key molecule that is positively correlated with tumor progression, but it remains unclear whether STAT1 is relevant to the malicious chemorefractory nature of USC. In the present study, we investigated the regulatory role of STAT1 toward platinum-cytotoxicity in USC. STAT1 suppression sensitized USC cells to increase cisplatin-mediated apoptosis ( $p < 0.001$ ). Furthermore, phosphorylation of STAT1 was prominently observed on serine-727 (pSTAT1-Ser727), but not on tyrosine-701, in the nucleus of USC cells treated with cisplatin. Mechanistically, the inhibition of pSTAT1-Ser727 by dominant-negative plasmid elevated cisplatin-mediated apoptosis by increasing intracellular accumulation of cisplatin through upregulation of CTR1 expression. TBB has an inhibitory effect on casein kinase 2 (CK2), which phosphorylate STAT1 at serine residues. Sequential treatment with TBB and cisplatin on USC cells greatly reduced nuclear pSTAT1-Ser727, enhanced intracellular accumulation of cisplatin, and subsequently increased apoptosis. Tumor load was significantly reduced by combination therapy of TBB and cisplatin in *in vivo* xenograft models ( $p < 0.001$ ). Our results collectively suggest that pSTAT1-Ser727 may play a key role in platinum resistance as well as tumor progression in USC. Thus, targeting the STAT1 pathway *via* CK2 inhibitor can be a novel method for attenuating the chemorefractory nature of USC.

## Introduction

Uterine serous carcinoma (USC) is characterized as a rare but aggressive subtype of endometrial cancer (EC). Most ECs are localized to the uterus at an early stage are well differentiated, and have a low histological grade. In contrast, USC accounts for a disproportionate 40% of total EC-related deaths, although it represents <10% of all EC.<sup>1</sup> Recently, due to its high recurrence rate, USC patients are usually treated with platinum-based adjuvant chemotherapy after surgical staging; however, many patients develop systemic recurrence, which is often life-ending.<sup>2</sup> Consequently, 72% of USC patients that develop recurrence die.<sup>3</sup> Thus,

resistance to platinum-based chemotherapy is a major issue for USC treatment, and it is urgent to reveal the associated underlying molecular mechanisms and to develop new treatment strategies to manage this complication.

Integrated genome-wide analysis revealed that USC has a characteristic molecular profile, completely distinct from that of endometrioid carcinomas, such as frequent *p53* and *p16* mutations, *HER2* overexpression, and *PIK3CA* amplification.<sup>4–6</sup> However, these genetic changes are also observed in intraepithelial carcinoma, and genuine driver genes that determine the aggressive nature and the poor prognostic outcome of USC are not well

**Key words:** STAT1, pSTAT1-serine (Ser727), casein kinase 2, copper transport protein, uterine serous carcinoma

**Abbreviations:** ANOVA: analysis of variance; ATP7B: ATPase copper transporting beta; CI: combination index; CK2: casein kinase 2; CTR1: copper transporter 1; Gy: gray; IC<sub>50</sub>: half maximal inhibitory concentration; IFN: interferon; MT2A: metallothionein 2A; NAC: neoadjuvant chemotherapy; Pt: platinum; SEM: standard error of the mean; Ser: serine; STAT1: signal transducer and activator of transcription 1; TBB: 4,5,6,7-tetrabromobenzotriazole; TCGA: the cancer genome atlas; Tyr: tyrosine; USC: uterine serous carcinoma

Additional Supporting Information may be found in the online version of this article.

**Conflict of interest:** The authors declare no competing interests.

**DOI:** 10.1002/ijc.32501

**History:** Received 23 Dec 2018; Accepted 24 May 2019; Online 10 Jun 2019

**Correspondence to:** Tsukasa Baba, MD, PhD, Department of Obstetrics and Gynecology, Iwate Medical University School of Medicine 19-1 Uchimarui, Morioka, Iwate, 020-8505, Japan, Tel.: +81-19-651-5111, Fax: +81-19-622-1900, E-mail: babatsu@iwate-med.ac.jp

**What's new?**

The molecular mechanisms underlying chemoresistance in uterine serous carcinoma (USC), a rare but highly aggressive subtype of endometrial cancer, remain unclear. This study shows that the prognostic outcome for USC patients with high STAT1 expression is poor and STAT1 is involved in platinum resistance. Mechanistically, cisplatin-induced STAT1 Ser727 phosphorylation alters cellular platinum accumulation to promote resistance and CK2 inhibitors can suppress STAT1 Ser727 phosphorylation. The results suggest that STAT1 could serve as a biomarker to predict tumor chemoresponse, and premedication with a CK2 inhibitor may represent a potent strategy to increase the efficacy of platinum-based chemotherapeutics in STAT1-high USC patients.

understood. Through genome-wide analysis and additional functional assays, we previously identified signal transducer and activator of transcription 1 (STAT1) as a multipotent molecule associated with several malignant characteristics of USC, such as proliferation, anchorage-independent growth, invasion, and tumorigenicity.<sup>7</sup> However, these traits are common of malignant tumors, and it remains unclear whether STAT1 directly determines the prognostic outcome of USC. The overall response rate (RR) of recurrent USC after platinum-based chemotherapy is 50%,<sup>2</sup> which indicates that USC could be classified as platinum-resistant or sensitive, and thus it is necessary to identify key molecules that modulate platinum-resistance. It is further presumed that STAT1 expression in USC enhances platinum resistance and that targeting this molecule could represent a new strategy to mitigate chemoresistance such as platinum resistance and improve disease outcome.

Cisplatin is among the most common chemotherapeutic drugs used for various cancers and EC. Its cytotoxic mechanism consists of the formation of DNA-damaging adducts and the subsequent induction of apoptosis and cell cycle arrest *via* multiple signaling pathways.<sup>8</sup> Cisplatin sensitivity in cancer cells is mainly attenuated by decreased DNA damage, enhanced DNA repair, reduced cellular accumulation of platinum and platinum inactivation.<sup>9,10</sup> It was reported that STAT1 suppression increases renal cell carcinoma sensitivity to cisplatin by regulating cell cycle arrest<sup>11</sup>; however, the molecular mechanism underlying the effect of STAT1 on platinum-resistance in USC remains unclear.

Thus, our aim was to determine whether and how high STAT1 expression functions in cisplatin-resistance in USC and to potentially uncover a new strategy to induce cisplatin susceptibility in USC.

**Materials and Methods****Cell lines and culture**

Human serous endometrial cancer cell lines included Spac1L (The Cancer Institute of the Japanese Foundation for Cancer Research, Japan), ARK1 and ARK2. ARK1 and ARK2 were generously provided in 2016 by Dr. A. Santin (Yale University, New Haven, CT) and were characterized in a previous report.<sup>12,13</sup> The human breast cancer cell lines, MCF7 and MD-MB-231 were kindly provided by the Department of Breast Surgery of Kyoto University. All cancer cell lines were grown in RPMI-1640 medium containing 10% fetal bovine serum (FBS) plus antibiotics at 37°C and 5% CO<sub>2</sub>.

**Western blot analysis**

Whole cell and nuclear lysates were prepared with RIPA lysis buffer (Thermo Scientific, Waltham, MA, #89900). Protein concentrations were determined using the BIO-RAD Quick Start Bradford protein assay (#500-0206) as standards. Cell-free extracts were frozen at -80°C. Cell lysates were denatured in 2× Laemmli Sample Buffer (BIO-RAD, #161-0737), heated to 95°C for 5 min, and loaded onto 8–12% SDS-gels. Separated proteins were transferred to Immobilon-P membranes (Millipore, #ISEQ10100) *via* semidry transfer. The membrane was then blocked with Blocking One Buffer (Nacalai Tesque, Kyoto, Japan, #03953-95) for 1 hr at room temperature, then washed three times with TBS-T, and incubated with primary antibodies at 4°C overnight as follows. STAT1 (D1K9Y) rabbit monoclonal antibody (mAb; CST, #14994), Phospho-STAT1 (Ser727) rabbit mAb (CST, #8826), phospho-Stat1 (Tyr701) rabbit mAb (CST, #9167), cleaved caspase-3 (Asp175) polyclonal antibody (pAb; CST, #9661), LC3A/B rabbit mAb (CST, #12741) and anti-GAPDH loading control rabbit mAb (CST, #2118) were obtained from Cell Signaling Technology (Danvers, MA). Anti-HDAC1 [ERR460] rabbit mAb (#ab109411), anti-DNA Ligase IV rabbit mAb (#ab193353), anti-Ku 70 rabbit pAb (#ab83501), anti-Ku 80 rabbit pAb (#ab87860) were from Abcam (Cambridge, MA). Anti-Rad51 (H-92) rabbit pAb (#sc-8,349), anti-FANCD2 (FI17) mouse mAb (#sc-20,022) and anti-MLH1 (C-20) rabbit pAb (#sc-582) were purchased from Santa Cruz Biotechnology (Dallas, TX). Anti-MSH2 mouse mAb (#NA27) was from Merck Millipore (Burlington, MA). GAPDH and HDAC1 were used as an endogenous loading control for whole cell lysis and nuclear lysis, respectively. All primary antibodies were used at 1:1,000 dilution and then incubated with appropriate horseradish peroxidase-conjugated secondary antibodies at 1:3,000 dilution at room temperature for 1 hr. Antirabbit IgG, HRP-linked antibody (CST, #7074) and antimouse IgG, HRP-linked (CST, #7076) antibodies were from Cell Signaling Technology. The signal was visualized using Chemi-Lumi One L Buffer (Nacalai Tesque, San Diego, CA, #07880-70).

**STAT1 knockdown**

STAT1 stably suppressed Spac1L cells were established by introducing *STAT1*-specific short hairpin RNA (shRNA) in the previous report.<sup>7</sup> Among the established nine clones, 89-C2 with least STAT1 expression was selected as shSTAT1 cells. By reconfirming the results of STAT1 suppression and functional assays with

dominant-negative *STAT1* DNA plasmid introduced cells, off-target effects were ruled out.<sup>7</sup>

#### Establishment of STAT1-phosphorylation mutants

The *STAT1* tyrosine (#12302, eGFP *STAT1* Y701F; *STAT1*, human Host: DH5alpha) and serine (#12303 eGFP *STAT1* S727A; *STAT1*, human Host: DH5alpha) mutant-encoding plasmids were purchased from Addgene (Tokyo, Japan). These plasmids were confirmed as previously described.<sup>14</sup> Ser727- and Tyr701-mutant plasmids were transfected with Lipofectamine 3000 (Thermo Fisher Scientific, Waltham, MA, #L3000-D15) to obtain p*STAT1* mutant cells. Stable transfectants were isolated by selection using 1 mg/ml G418 (Nacalai Tesque, #16513-84).

#### Xenograft models

Female nonobese diabetic/severe combined immunodeficient (NOD/SCID) mice and BALB/c nude mice were purchased from Nihon Clea (Tokyo, Japan). Xenograft models were initiated by the subcutaneous injection of Spac1L ( $5 \times 10^6$ ) and ARK2 ( $2 \times 10^6$ ) cells suspended in approximately 200  $\mu$ l of a 1:1 medium:Matrigel solution into the right flank of each mouse (NOD/SCID mice with Spac1L, BALB/c nude mice with ARK2). Tumor volumes were measured twice weekly. Tumor volumes were calculated using the formula: tumor volume ( $\text{mm}^3$ ) =  $(W^2 \times L)/2$ , where  $W$  is width and  $L$  is length in mm. Given ethical considerations, mice inoculated with Spac1L cells or ARK2 cells were sacrificed 6 or 4 weeks after inoculation, respectively; thus tentative survival rates were determined by designating the mice with tumor burdens in excess of 150 $\text{mm}^3$  as near death from disease.

#### Immunohistochemistry staining of STAT1 and pSTAT1-Ser727 in human tissues

Immunohistochemistry (IHC) was performed to detect of *STAT1* and p*STAT1* Ser727 expression in patient samples, as previously described.<sup>7</sup> Tissue sections were incubated with primary antibody including, *STAT1* (D1K9Y) rabbit mAb (CST, #14994) diluted at 1:3,000 or phospho-*STAT1* (Ser727) rabbit mAb (CST, #8826) diluted 1:800 for overnight at 4°C, and then stained with HRP-conjugated secondary antibodies (NICHIREI Biosciences Inc., Tokyo, Japan, Histofine SAB-Po kit, #424032). DAB (Sigma, St. Louis, MO, #D4418) was used to visualize peroxidase activity. Hematoxylin staining used as a counterstain. Human tonsil tissue was used as a *STAT1*-positive control, whereas human breast cancer tissue was a positive control for p*STAT1*-Ser727.

To analyze IHC results, semiquantitative methods were employed. In detail, *STAT1* and p*STAT1* IHC scores were calculated by combining staining intensity with percent positive areas. Staining intensity ranged from 0 to 3 (0: negative; 1, weak; 2, moderate; 3, strong). The percent-positive staining areas in tumors were calculated using a scale of 0–4 (0, <5%; 1, 5–25%; 2, 25–50%; 3, 50–75%; 4, >75%).

For each tumor, the percentage of DAB-positive staining was evaluated in four different areas.

#### Statistical analysis

For all experiments, quantitative data are presented as mean  $\pm$  SEM from three independent experiments. All statistical analyses were performed using GraphPad Prism 7.0 (GraphPad Software, San Diego, CA). Data were analyzed by Student's *t*-test and two-way ANOVA analysis. Statistical significance was defined as follows: \* $p < 0.05$ ; \*\* $p < 0.005$ ; \*\*\* $p < 0.001$  (as compared to controls).

Precise experimental procedures were described in the file of Supporting Information Materials and Methods.

#### Results

##### High STAT1 expression is associated with poor prognostic outcome for USC patients

To assess the relationship between *STAT1* expression and USC prognosis, we investigated *STAT1* expression by immunohistochemistry ( $n = 40$ ). According to our previous study,<sup>7</sup> *STAT1* IHC scores are presented as 0–4. Tumor with high *STAT1* expression (scores of 2–4) were associated with significantly reduced overall survival ( $p < 0.01$ ) and progression-free survival ( $p < 0.01$ ) compared to those with low *STAT1* expression (scores of 0 and 1; Figs. 1a and 1b). Clinicopathological analysis based on *STAT1* expression is summarized in Table 1. Individuals with high *STAT1* expression exhibited a higher relapse rate ( $p < 0.005$ ), although almost 90% of patients underwent adjuvant chemotherapy. Similarly, survival outcomes of USC patients with high *STAT1* mRNA expression were lower in a TCGA cohort ( $p = 0.1372$ ; Supporting Information Fig. S1a). As USC is highly resistant to chemotherapy,<sup>7</sup> and especially resistant to cisplatin, we hypothesized that high *STAT1* expression might be related to cisplatin-resistance.

##### STAT1 may confer resistance to cisplatin in USC cells

To clarify the chemoresistant role of *STAT1* in USC, the chemosensitivity of Spac1L cells was assessed with or without *STAT1* knockdown. In *STAT1* knockdown (sh*STAT1*) cells, *STAT1* protein and mRNA expression were suppressed compared to that in Mock cells (Fig. 2a and Supporting Information Fig. S1b). IC<sub>50</sub> assays indicated that loss of *STAT1* leads to increased cisplatin sensitivity (Fig. 2b). Increased sensitivity to two additional DNA-damaging agents, irinotecan and doxorubicin, but not to paclitaxel, was also observed (Supporting Information Fig. S1c).

To confirm these observations, we compared *STAT1* expression and cisplatin sensitivity among three USC cell lines: Spac1L, ARK1 and ARK2. *STAT1* was highly expressed in ARK2 and Spac1L cells (Fig. 2c, Supporting Information Fig. S1d), and high *STAT1*-expressing cells were more resistant to cisplatin (Fig. 2d, Supporting Information Fig. S1e). Apoptosis was increased in sh*STAT1* cells even with low-dose cisplatin treatment (Supporting Information Fig. S1f). This was confirmed by cleaved-caspase 3 assays in Mock/sh*STAT1* cells and Spac1L/ARK1/ARK2 cells, respectively (Fig. 2e, Supporting Information Fig. S1g). Together, these data suggest that *STAT1* might play an important role in cisplatin chemosensitivity in USC cells.

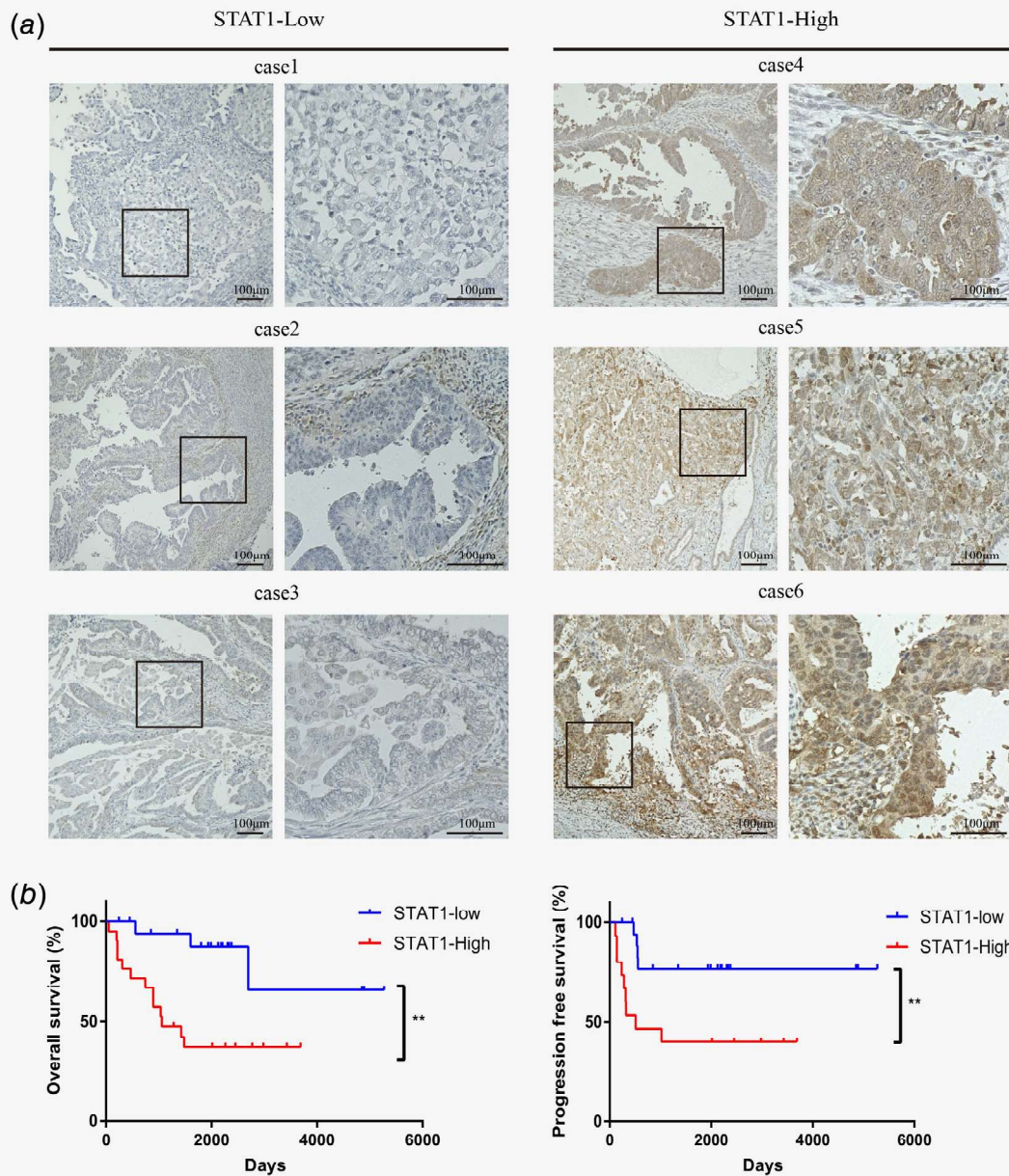


**Figure 1.** High STAT1 expression is associated with poor prognostic outcome of patients bearing uterine serous carcinoma. (a) Representative micrographs of STAT1 IHC staining in uterine serous carcinoma (USC). The expression of STAT1 in USC ( $n = 40$ ) was assessed with stained intensity (0–4) and stained area (%) as previously reported.<sup>7</sup> Based on STAT1 expression score, USC patients were divided into two groups: STAT1-high, score  $\geq 2$  ( $n = 21$ ); STAT1-low, score  $< 2$  ( $n = 19$ ). Representative three groups of micrographs captured under (Left panel) low magnification (20 $\times$ ) and (Right panel) high magnification (40 $\times$ ) were exhibited respectively. Scale bars indicate 100  $\mu\text{m}$ . (b) Kaplan–Meier analysis of overall survival (OS) curves and progression free survival (PFS) curves in 40 USC patients. Comparison of OS and PFS between STAT1-high patients and STAT1-low patients was performed the log-rank test (\*\*0.001  $< p < 0.01$ ). [Color figure can be viewed at wileyonlinelibrary.com]

### Sensitivity of shSTAT1 cells to cisplatin is correlated with DNA damage

DNA-damaging agents have been readily used for cancer chemotherapy. Chemotherapeutics target rapidly dividing cancer cells by directly or indirectly inducing DNA damage. H2AX histone

phosphorylation ( $\gamma$ -H2AX) is an early response to DNA damage in mammals.<sup>15</sup> Immunofluorescent staining for  $\gamma$ -H2AX enhanced H2AX focus formation (green) in shSTAT1 cells compared to that in Mock cells under the treatment with 1  $\mu\text{M}$  cisplatin (Fig. 2f). Flow cytometric (FACS) analysis further confirmed the significant

**Table 1.** Clinical characteristics of 40 uterine serous carcinoma patients in STAT1 IHC analysis

|                        | STAT1-low     | STAT1-high    | p-value |
|------------------------|---------------|---------------|---------|
| Characteristic         | Low (<2)      | High (≥2)     |         |
| Number                 | 19            | 21            |         |
| IHC score              | <2            | ≥2            |         |
| Age (years)            | 67 ± 3.6      | 63 ± 1.8      | 0.3742  |
| Median survival (days) | 4,851         | 1,601         | 0.0044  |
| FIGO Stage             |               |               |         |
| I and II               | 10            | 6             | 0.1965  |
| III and IV             | 9             | 15            |         |
| Chemotherapy           | 72.2% (13/18) | 88.2% (15/17) | 0.4018  |
| Relapse                | 21.1% (4/19)  | 75% (12/16)   | 0.0022  |

increase in cisplatin-induced DNA damage in shSTAT1 cells (Supporting Information Fig. S1h). These results suggested that STAT1 modulates cisplatin-induced DNA damage.

#### STAT1 is not engaged in the DNA damage repair process during cisplatin-induced cell death

There are many factors that modulate the efficacy of cisplatin therapy such as DNA repair, drug uptake and efflux and drug inactivation.<sup>16</sup> To identify the factors involved in platinum resistance, Mock and shSTAT1 cells treated with cisplatin were used to assess DNA repair pathways such as the homologous recombination (HR) pathway,<sup>17,18</sup> nonhomologous end joining (NHEJ) pathway,<sup>19</sup> FANCD2 crosslink pathway,<sup>20</sup> mismatch pathway,<sup>21</sup> and nucleotide excision repair (NER) pathway.<sup>22</sup> For the HR pathway, nuclear Rad51 foci in Mock and shSTAT1 cells were assessed with or without 1 μM cisplatin treatment for 24 hr by immunostaining and western blotting. Nuclear Rad51 foci numbers did not change between Mock and shSTAT1 cells upon cisplatin treatment, and no significant difference in nuclear Rad51 expression was found by western blotting after cisplatin (Supporting Information Fig. S2a).

Regarding the NHEJ pathway, no significant differences in protein levels of DNA ligase IV, Ku70 and Ku80 were found compared between Mock and shSTAT1 USC cells, with or without cisplatin treatment (Supporting Information Fig. S2b).

Next, we analyzed the correlation between the FANCD2 crosslink pathway status and STAT1 expression. Upon assessing the mono-ubiquitination status of FANCD2 (Ub-FANCD2) after cisplatin treatment, a slightly higher level of ubiquitination FANCD2 was observed in shSTAT1 cells by western blotting, although this was not prominent (Supporting Information Fig. S2c).

Regarding the mismatch pathway, remarkable differences in MSH2, MLH1 and PolB levels between Mock and shSTAT1 cells were not found (Supporting Information Fig. S2d).

Finally, we determined whether the NER pathway was involved in STAT1-mediated cisplatin resistance. The expression

of ERCC1, ERCC2, ERCC3, XPA and XPF were evaluated in USC cells, but none were activated in Mock and shSTAT1 cells upon cisplatin treatment (Supporting Information Fig. S2e).

Furthermore, H2AX expression in shSTAT1 and Mock cells was assessed by flow cytometry after irradiation (IR),<sup>23</sup> but there were no significant changes between in Mock and shSTAT1 cells in response to irradiation exposure (Fig. 2g). Together, DNA repair pathways do not seem to be involved in STAT1-related cisplatin resistance in USC cells.

#### Intracellular cisplatin accumulation increases in shSTAT1 cells

To identify the mechanism related to cisplatin resistance, other than DNA repair, we next investigated cellular accumulation of cisplatin in USC cells using an anticisplatin modified DNA complex antibody (anti Pt-DNA) followed by dot-blot assays and flow cytometry. After 20 μM cisplatin treatment for 24 hr, an increased number of Pt-DNA-positive cells was observed in the shSTAT1 group (16.9%), compared to that in the Mock (7.9%;  $p < 0.001$ ; Fig. 2h). Dot blot assays also showed a significant increase in the Pt-DNA complex in shSTAT1 cells (Supporting Information Fig. S3a). Similarly, intracellular Pt-DNA accumulation was significantly enhanced in ARK1 cells along with increasing cisplatin concentration (10–86.4%), while this enhancement was weaker in Spac1L cells (1.3–10.4%) and almost not observed in ARK2 cells (0.2–0.56%, Supporting Information Fig. S3b). These data suggest that cisplatin cellular accumulation is inhibited by STAT1.

Copper transporter 1 (CTR1) is a mediator of cisplatin influx<sup>24,25</sup> and functions in its mature form.<sup>26</sup> CTR1 mRNA expression was significantly lower in Mock cells ( $p < 0.05$ ; Supporting Information Fig. S3c). Western blot analysis demonstrated that mature CTR1 is expressed at low levels in Mock cells, with higher levels confirmed in shSTAT1 cells after cisplatin exposure (Supporting Information Fig. S3d). This CTR1 suppression was observed by FACS in Mock cells treated with cisplatin, while not in shSTAT1 cells ( $p < 0.005$ ; Supporting Information Fig. S3e). Moreover, ATP7B, an exporter of cisplatin,<sup>27</sup> and MT2A, a cisplatin inactivator,<sup>28</sup> were upregulated in Mock cells (Supporting Information Figs. S3f and S3g).

#### Cisplatin prompts USC cells to phosphorylate at serine, but not tyrosine of STAT1

C188-9, a STAT1 inhibitor, was expected to be effective against STAT1-high tumors<sup>29</sup>; however, cellular viability or apoptosis in Spac1L cells was not remarkably altered by C188-9 (data not shown). STAT1 functions as a transcription factor *via* phosphorylation at serine-727 or tyrosine-701 to translocate, which induces translocation to the nucleus.<sup>30,31</sup> STAT1 phosphorylation was assessed using nucleolus extracts from Mock and shSTAT1 cells by western blotting. Although both serine (Ser727) and tyrosine (Tyr701) phosphorylation were observed with IFN treatment, there was a significant increase in serine, but not tyrosine phosphorylation upon cisplatin treatment (Fig. 3a). Similarly, in ARK2 cells with prominent STAT1 expression, STAT1 serine

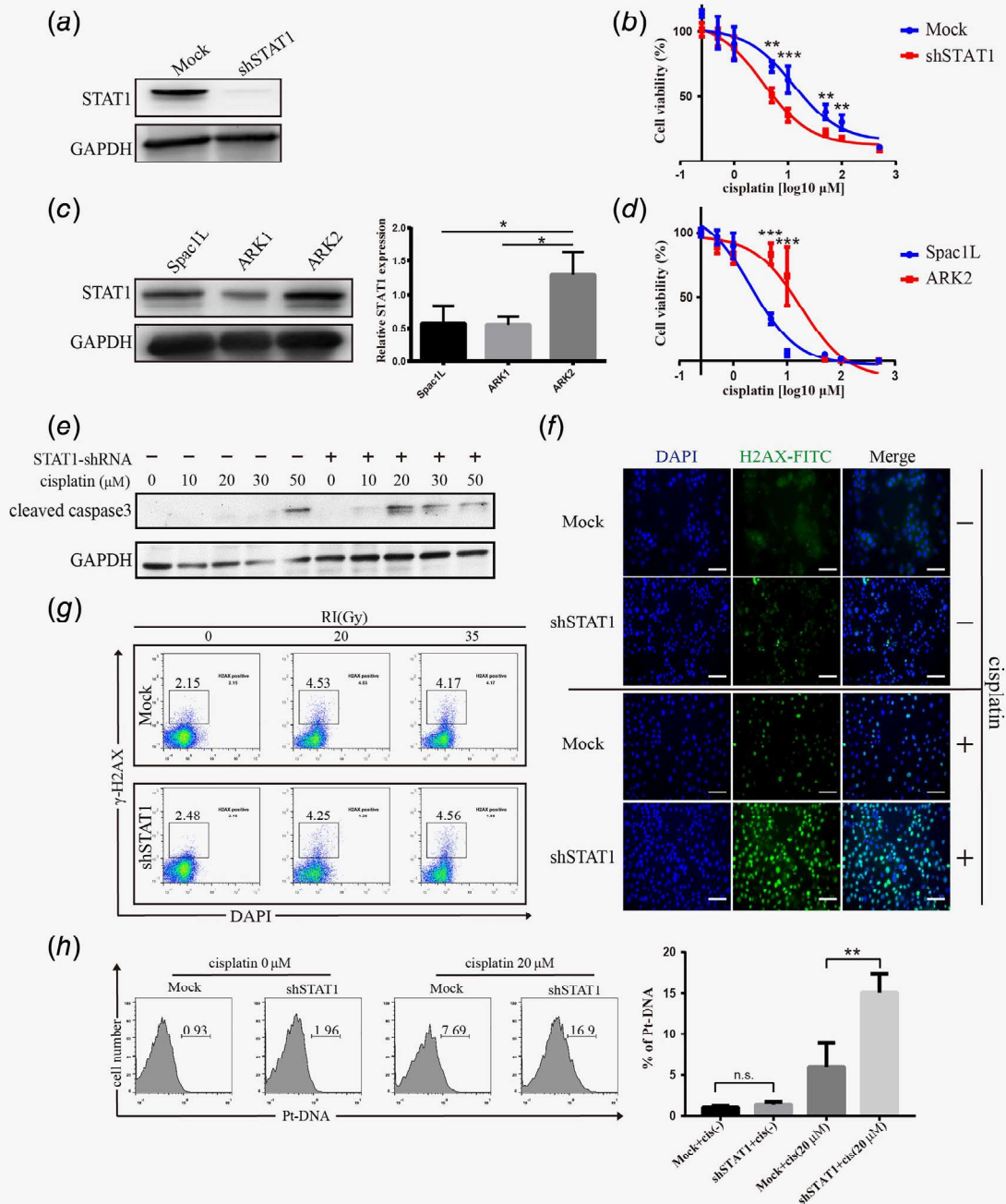


**Figure 2.** STAT1 expression status and chemosensitivity of USC cell lines to cisplatin. (a) STAT1 expression on Spac1L cells which were stably transfected with control vector (Mock) and STAT1 shRNA. (b) Cisplatin IC<sub>50</sub> assay of Mock cells and shSTAT1 cells treated with several doses of cisplatin for 72 hr (\*\*0.001 < *p* < 0.01; \*\*\**p* < 0.001). (c) STAT1 expressing status of three USC cell lines, Spac1L, ARK1 and ARK2, was confirmed by western blot quantification. Error bar represent SEMs for three independent experiments (\**p* < 0.05). (d) Cisplatin IC<sub>50</sub> assay of Spac1L and ARK2 cells treated with cisplatin for 72 hr (\**p* < 0.05; \*\*0.001 < *p* < 0.01; \*\*\**p* < 0.001). (e) Apoptotic status of Mock and shSTAT1 cells were assessed after 24 hr cisplatin treatment in several doses (10, 20, 30 and 50 μM). Cleaved caspase-3 expression was determined by western blot analysis (\**p* < 0.05; \*\*0.001 < *p* < 0.01; \*\*\**p* < 0.001). (f) DNA damage status of Mock and shSTAT1 cells with or without cisplatin treatment (1 μM) for 24 hr were assessed by immunofluorescent staining of γ-H2AX (green). Nuclei were visualized by DAPI (blue). Images were captured under 200× magnification. Scale bar = 80 μm. (g) DNA damage status (γ-H2AX expression) of Mock and shSTAT1 cells after several doses of IR exposures (0, 20 or 35 Gy) assessed by flow cytometry. (h) Flow cytometric analysis of cisplatin-DNA complex presentation, % Pt-DNA of Mock and shSTAT1 cells sequentially exposed to cisplatin 20 μM for 24 hr (\*\*0.001 < *p* < 0.01). The bar graphs represent mean + SEM for three independent experiments. [Color figure can be viewed at [wileyonlinelibrary.com](http://wileyonlinelibrary.com)]

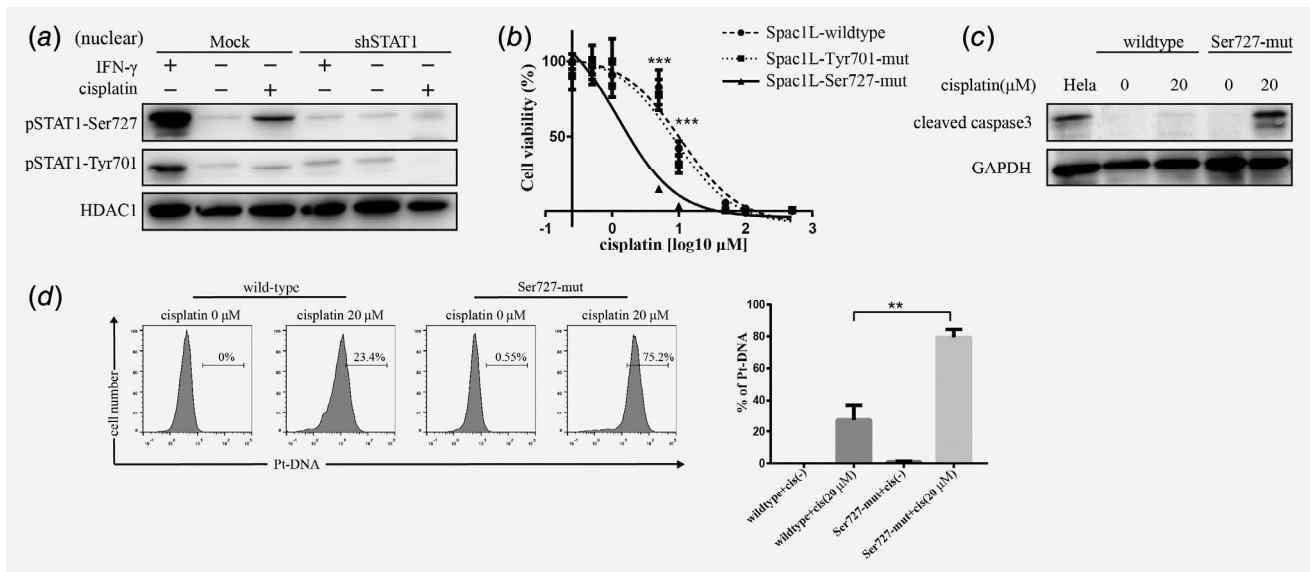


**Figure 3.** Serine phosphorylated STAT1 plays a crucial role in cisplatin resistance of USC cells. (a) STAT1 phosphorylation status at serine residue or tyrosine residue (pSTAT1-Ser727 or pSTAT1-Tyr701) of nuclear fraction of Mock and shSTAT1 cells after exposure to IFN- $\gamma$  or Cisplatin for 24 hr were assessed by western blot analysis. (b) Cisplatin IC<sub>50</sub> of Spac1L wild-type cells, Tyr701-mut and Ser727-mut cells (\*\**p* < 0.001). (c) Cisplatin induced apoptosis was assessed by expression of cleaved caspase-3 in Spac1L wild-type cells and Ser727-mut cells using western blot analysis. Hela cells were used as a positive control (\*\**p* < 0.001). (d) Nuclear accumulation of cisplatin in Spac1L wild-type cells and Ser727-mut cells were assessed by flow cytometry analysis (\*\**p* < 0.001). The bar graphs present the mean + SEM for three independent experiments.

phosphorylation was observed after cisplatin treatment, decreased under the pretreatment of TBB followed by cisplatin (Supporting Information Fig. S6c). These results indicated that cisplatin prompts USC cells to phosphorylate at STAT1 serine, but not tyrosine.

#### pSTAT1 serine-mutant promotes cisplatin-mediated apoptosis and cisplatin cellular accumulation

Based on these results, we hypothesized that cisplatin stimulates STAT1 phosphorylation at serine residue resulting in altered cytotoxic activity upon platinum therapy in USC cells. To test this hypothesis, dominant-negative assays were conducted. First, we transfected serine-mutant (Ser727-mut) or tyrosine-mutant (Tyr701-mut) plasmid in Spac1L cells. We then picked the clones with the lowest expression of serine phosphorylation (Ser727-mut-A1) and tyrosine phosphorylation (Tyr701-mut-C2) mutants (Supporting Information Fig. S4a). Based on IC<sub>50</sub> assays, Ser727-mut cells were tremendously sensitive to cisplatin compared to sensitivity with Tyr701-mut or spac1 control cells (*p* < 0.0001) (Fig. 3b). Moreover, Ser727-mut cells were more apoptotic upon cisplatin treatment (Fig. 3c). With cisplatin administration, Ser727-mut cells exhibited a nearly fourfold increase in Pt-DNA accumulation (*p* < 0.001; Fig. 3d). These results were confirmed in ARK2 USC cells (Supporting Information Figs. S4b–S4e). In both Spac1L and ARK2 cells, expression of serine-mutant resulted in significantly higher CTR1 expression compared to that in wild-type cells (Supporting Information Figs. S4f and S4g). Together, these results suggest

that cisplatin induces STAT1 serine phosphorylation in USC cells suppress cisplatin accumulation.

#### Phosphorylation of STAT1 at serine is not directly involved in the autophagic process

Autophagy is another known chemoresistant process. To evaluate whether cisplatin induces autophagy *via* STAT1 phosphorylation at serine, a LC3 turnover assay was conducted. Under cisplatin treatment, a certain autophagy activity marker, LC3B was expressed not only in Spac1L and ARK2 cells but their Ser727-mut cells or shSTAT1 cells, and there was no definite association between LC3B expression and cisplatin-resistance among these cells (Supporting Information Fig. S5). Chloroquine (CQ) attenuated LC3B expression of USC cells with or without pSTAT1 as an autophagy inhibitor.

#### CK2 inhibition suppresses cisplatin-induced STAT1 serine phosphorylation in USC cells

To expand the potential clinical antitumor application of anti-STAT1 strategies, we examined an available pharmacological inhibitor of STAT1 serine phosphorylation. Serine/tyrosine phosphatases, such as p38, ERK1/2, phosphatidylinositol 30-kinase (PI3K), Ca/calmodulin-dependent protein kinase II (CaMKII) and protein kinase C (PKC) can induce STAT1 phosphorylation in various tumor cells.<sup>32–36</sup> SB203580, KN-62 and H7 were chosen to inhibit p38, CaMKII and PKC to assess whether cisplatin-induced Ser727 phosphorylation could be suppressed. As shown in Supporting Information Figure S6a, Ser727 phosphorylation

after cisplatin combination treatment in Spac1L cells was not suppressed by p38, CaMKII and PKC inhibitors. In contrast, as shown by immunostaining (Fig. 4a and Supporting Information

Fig. S6b), cisplatin-induced nuclear Ser727 phosphorylation in Spac1L cells was significantly inhibited by TBB, a serine-threonine kinase II casein kinase2 (CK2) inhibitor.<sup>37-39</sup> As

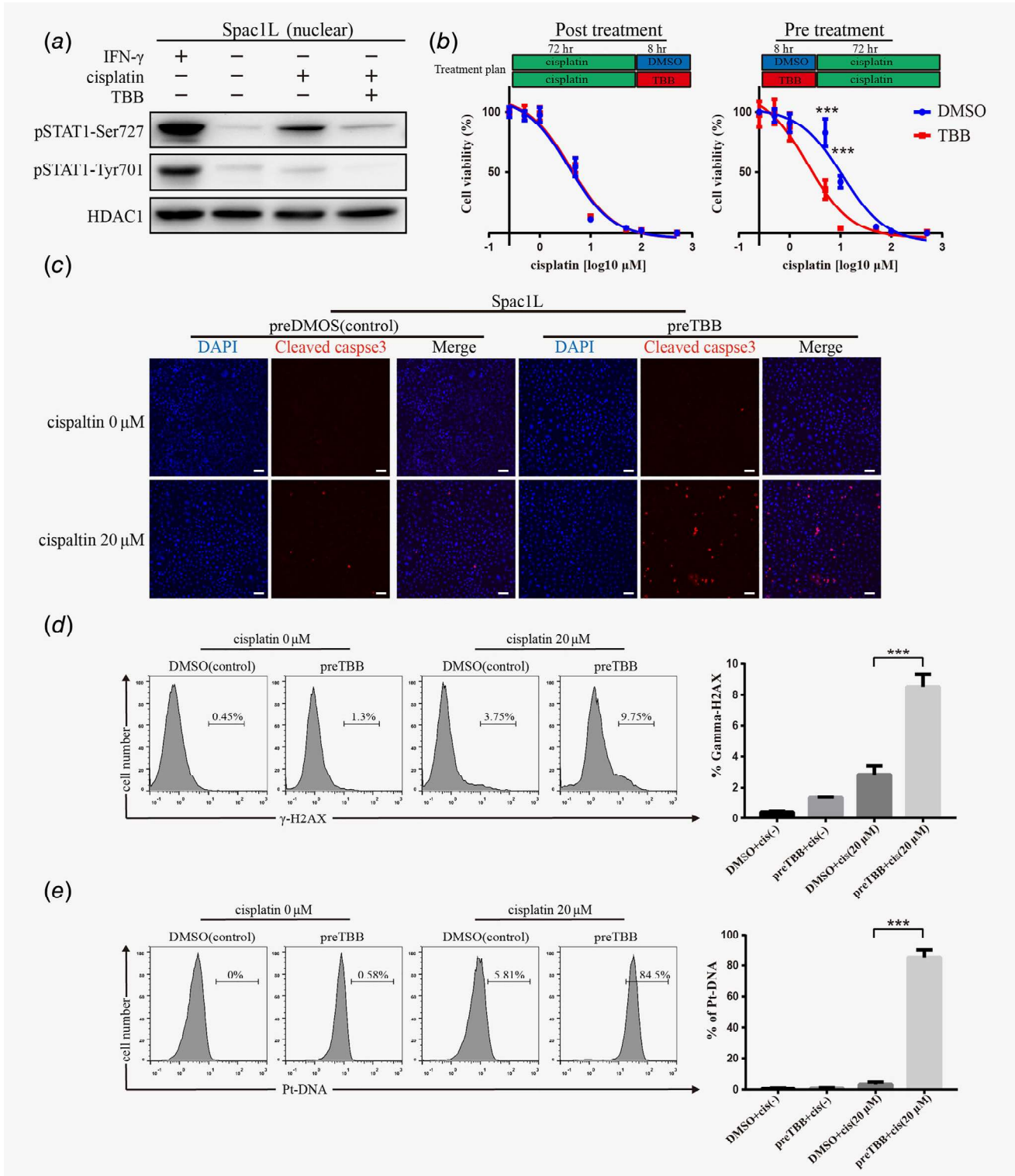


Figure 4. Legend on next page.



epidermal growth factor receptor (EGFR) is upstream of STAT1, EGFR inhibitors are also expected to be effective; accordingly, gefitinib moderately attenuated STAT1 Ser727 phosphorylation (data not shown).

TBB pretreatment (preTBB) at 50  $\mu\text{M}$  for 8 hr before cisplatin, but not posttreatment, significantly reduced cell viability (Fig. 4b). To verify the apoptotic effect of preTBB combination therapy, Spac1L cells were pretreated with TBB or DMSO (as control) for 8 hr, followed by cisplatin treatment. Upregulation of cleaved-caspase3 foci was observed in preTBB cells based on immunofluorescence (Fig. 4c). Consistent with these results, the same effect of suppressing Ser727 phosphorylation in ARK2 cells was also reproduced by TBB pretreatment and cisplatin (Supporting Information Fig. S6c–S6e). The DNA damage marker H2AX was significantly elevated after preTBB and cisplatin combination treatment (Fig. 4d). Importantly, TBB pretreatment with cisplatin significantly increased Pt-DNA adducts, compared to that with cisplatin alone (Fig. 4e). These results suggest that TBB pretreatment can significantly suppress cisplatin-induced Ser727 phosphorylation and attenuated STAT1-related cisplatin resistance in USC. TBB was not cytotoxic, as there was no significant reduction in cell survival with 50  $\mu\text{M}$  TBB pretreatment alone (Supporting Information Fig. S6f). The combination index was assessed for cisplatin and TBB pretreatment using the Chou–Talalay method.<sup>40</sup> As CI value was below 1 (Supporting Information Fig. S6g), a synergistic effect was confirmed. In addition, this synergic cytotoxic effect was observed in MB-MDA-231 and MCF7 breast cancer cell lines (Supporting Information Figs. S7a and S7b). Given these findings, we conceived that pretreatment with TBB to target CK2 kinase for suppressing STAT1 Ser727 phosphorylation could be a potential strategy to attenuate cisplatin resistance in cancer cells.

#### STAT1-Ser727 phosphorylation mediation with CK2 inhibitor followed by cisplatin is effective on *in vivo* tumor growth of cisplatin-resistant USC cells

As previously described, we expected that high-STAT1 related cisplatin resistance can be dissolved by suppressing STAT1-Ser727 phosphorylation *via* combining a CK2 inhibitor. To investigate the antitumor effect of CK2 inhibitor, TBB and cisplatin combination therapy, we used Spac1L and ARK2 xenograft mouse models. First, as TBB was designated only for *in vitro* experimental use, the highest safe dose of TBB in mouse experiments was determined. The *in vivo* toxicity assessment was performed on nude mice, which were administered various doses of

TBB (1, 2 and 3 mg), and body weight was measured daily. As shown in Supporting Information Figure S8a, there was no remarkable change in body weight by a 1 mg daily administration of TBB, which was determined as the safe dose. In Spac1L xenograft mice, pretreatment with TBB from Day 14 to 21 followed by cisplatin treatment significantly inhibited Spac1L tumor growth, and tumors became undetectable even at 40 days ( $p < 0.0001$ ) as compared to the DMSO group (Fig. 5a, Supporting Information Fig. S8b). The 6 weeks survival rates were 100 and 67% in preTBB and DMSO groups, and the representative Spac1L xenograft tumors in each group were shown in Figure 5a right panel. In ARK2 xenograft mice, the tumor growth in mice pretreated with TBB was almost suppressed by cisplatin treatment, while not in mice without TBB pretreatment ( $p < 0.0001$ ; Fig. 5b, left panel). Furthermore, the tumor growth in ARK2 Ser727-mut bearing mice was significantly inhibited by cisplatin treatment compared to wild-type ARK2 bearing mice ( $p < 0.0001$ ; Fig. 5b, right panel). The 4 weeks survival rates of ARK2 xenograft mice were 100% in the STAT1 Ser727 phosphorylation mediated groups, while not without mediation (Supporting Information Fig. S8b). These data suggested that inhibition of STAT1 Ser727 phosphorylation by TBB prior to cisplatin treatment exerts a significant antitumor effect.

#### Phosphorylation of STAT1 at serine is observed in USC patients after neoadjuvant chemotherapy (NAC)

To evaluate whether cisplatin induces STAT1 phosphorylation at serine in human disease, immunohistochemistry staining was conducted using specimen from USC patients with or without chemotherapy administration prior to surgery, termed NAC. Intriguingly, serine phosphorylation of STAT1 serine was only observed in specimens from USC patients who underwent NAC and not in those from NAC-untreated USC patients, even when STAT1 expression was detected. Furthermore, STAT1 serine phosphorylation was more prominent in metastatic nodes (Fig. 5c, Supporting Information Fig. S9).

#### Discussion

USC is designated as the most aggressive subtype of EC and is associated with poor prognostic outcomes. It is necessary to identify key molecules that modulate platinum-resistance, and we hypothesized that targeting STAT1 might provide a potent strategy to overcome platinum resistance in USC, in order to improve clinical outcomes. In our study, we demonstrated endogenous STAT1 expression in USC and determined that it

**Figure 4.** TBB, a CK2 inhibitor, can significantly suppress STAT1 serine phosphorylation to increase sensitivity in USC cells to cisplatin. (a) Nuclear STAT1 phosphorylation status of Spac1L cells sequentially treated with TBB (50  $\mu\text{M}$  for 8 hr) and cisplatin (20  $\mu\text{M}$  for 24 hr) were assessed by western blotting. (b) Cisplatin  $\text{IC}_{50}$  assays of Spac1L cells with posttreatment or pretreatment of TBB (50  $\mu\text{M}$  for 8 hr) or DMSO. Bar graphs above figures represent time course of treatment plan of preexperiment and postexperiment. (c) Cisplatin induced apoptosis was immunohistochemically assessed by expression of cleaved caspase-3 (red) in Spac1L cells, with or without TBB pretreatment (50  $\mu\text{M}$  for 8 hr). Nucleus was stained with DAPI (blue). Scale bar = 80  $\mu\text{m}$ . (d, e) Flow-cytometry analysis of DNA damage biomarker,  $\gamma$ -H2AX expressing population (d) and cisplatin-DNA complex presentation, % Pt-DNA (e) of Spac1L cells sequentially treated with TBB and cisplatin ( $***p < 0.001$ ). The bar graphs represent the mean + SEM for three independent experiments. [Color figure can be viewed at [wileyonlinelibrary.com](http://wileyonlinelibrary.com)]

plays a role in platinum sensitivity. High STAT1 expression is also a hallmark of poor outcome in breast cancer but in leukemia is associated with good susceptibility to chemotherapy or

radiotherapy,<sup>31,41</sup> and suppressing STAT1 leads to an increased cytotoxic response.<sup>11,42</sup> These findings imply that STAT1 is a master regulator of chemosensitivity; however, how STAT1

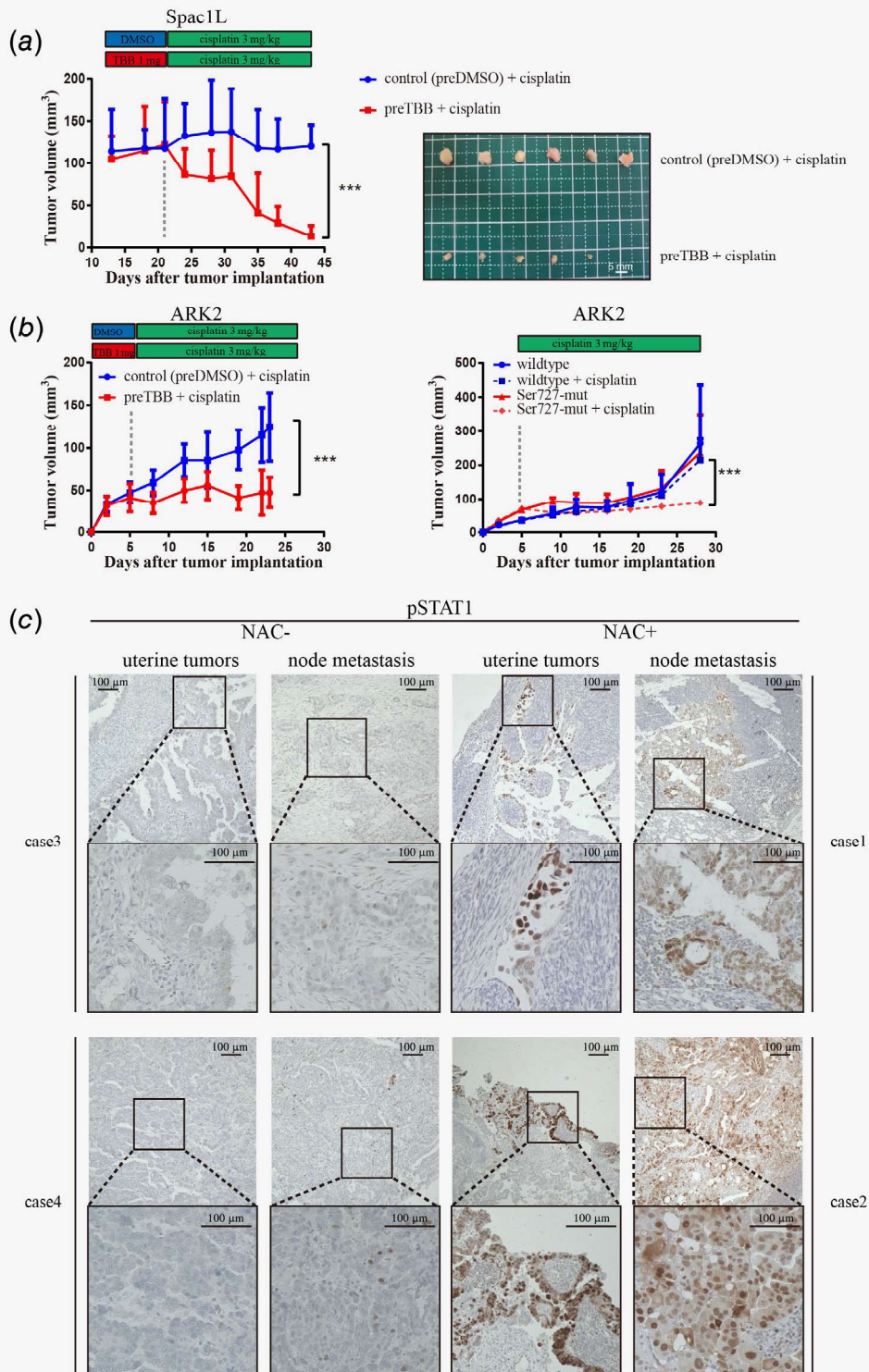
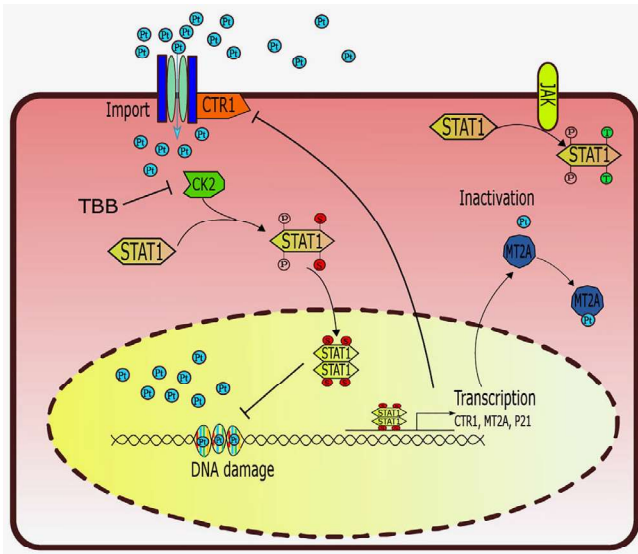


Figure 5. Legend on next page.



**Figure 6.** Schematic illustration showing the role of the CK2/pSTAT1-Ser727/CTR1 axis in cisplatin resistance mechanism in USC. [Color figure can be viewed at [wileyonlinelibrary.com](http://wileyonlinelibrary.com)]

functions in the complex mechanism of platinum-resistance were previously unclear.

Resistance to cisplatin is based on several mechanisms such as decreased DNA damage, enhanced DNA repair, reduced cellular accumulation of platinum and platinum inactivation. Among these, HR is a key pathway in DNA repair for variety of cancers<sup>17</sup>; moreover, nuclear Rad51 foci formation is a hallmark of the HR DNA repair pathway.<sup>18</sup> NNHEJ and FANCD2 crosslinking also play important roles in regulating the signal from BRCA1 and Rad51 to induce downstream repair pathways.<sup>20,43</sup> Further, high expression of NER genes is associated with cisplatin resistance in human ovarian, lung, and testicular cancer.<sup>22,44,45</sup> However, these DNA damage repair systems were not significantly induced in STAT1-high USC cells (Supporting Information Fig. S2). Moreover, even irradiation, which can directly generate DNA double-strand breaks in cancer cells,<sup>23</sup> did not alter H2AX expression in USC cells with or without high STAT1 expression (Fig. 2g). Compared to the high frequency of homologous recombination deficiency (HRD) in high-grade serous ovarian cancer,<sup>46</sup> such genetic alterations are not observed as frequently in USC.<sup>26,47</sup> These results

suggest that in USC, platinum-susceptibility is determined not by HR status but by other mechanisms, such as STAT1-oriented resistance. In support of this notion, STAT1 deficiency sensitized USC cells to cisplatin by altering cellular cisplatin accumulation partially through mature CTR1 (Supporting Information Figs. S3c and S3d), CTR1 delivers cisplatin into the cell *via* chelation by the N-terminal domain, which is followed by endocytosis of platinum-based drugs<sup>26</sup>; accordingly, overexpression of CTR1 can attenuate cisplatin resistance by increasing intracellular concentrations.<sup>24,25,48</sup> Intracellular cisplatin accumulation is also maintained by an exporter and an inactivator. ATP7B is a cisplatin exporter and is highly expressed in cisplatin-resistant cancer cells,<sup>27,48</sup> whereas MT2A detoxifies heavy metals in tumor cells and its overexpression confers cisplatin resistance.<sup>28,49</sup> Significant changes in MT2A, but not ATP7B, were observed with STAT1 knockdown (Supporting Information Figs. S3f and S3g), suggesting that MT2A is associated with STAT1-related cisplatin resistance. As CTR1 and MT2A were enhanced in STAT1-suppressed USC cells exposed to cisplatin, STAT1 might modulate cisplatin resistance by regulating platinum influx and inactivation.

In addition to the above well-known mechanism of cisplatin resistance, it is also known that autophagy is involved in cell death and chemoresistance processes. In ovarian cancer, autophagy was induced by cisplatin,<sup>50</sup> and LC3B is considered a biomarker indicating autophagy. In our study, there was no definite association between LC3B expression and STAT1-Ser727 status as well as cisplatin-resistance in USC cell lines (Supporting Information Fig. S5). These results suggested that autophagy may not play the dominant role in STAT1-cisplatin resistance. However, regarding CQ attenuated LC3B expression, it is possible that autophagy is partially involved in platinum resistance of USC *via* other than STAT1 signal.

STAT1 modulates its downstream pathways *via* phosphorylation at Ser727 or Tyr701. Generally, STAT1 is designated to work as a tumor suppressor that is involved in the JAK/STAT1 death signaling pathway, *via* phosphorylation at Tyr701; however, little is known about at Ser727 phosphorylation in tumor progression. In our study, the use of a dominant negative STAT1 phosphorylation mutant demonstrated that cisplatin treatment induces STAT1 phosphorylation at Ser727 in USC cells to suppress platinum uptake and apoptosis (Fig. 3 and Supporting Information

**Figure 5.** Functional roles of serine-phosphorylated STAT1 in chemosensitivity to cisplatin treatment. (a) TBB pretreatment increased antitumor effect of cisplatin *in vivo*. NOD-SCID mice were subcutaneously inoculated with  $5 \times 10^6$  Spac1L cells. Tumor growth in mice treated with cisplatin (3 mg/kg BW, twice a week) was compared between groups preadministered with TBB (1 mg, once per day for 7 days) or DMSO. DMSO was used as placebo control. Excised tumors were set in two rows of representative image (top, DMSO-pretreated; bottom, TBB-pretreated). Statistical analysis was performed two-way ANOVA analysis ( $***p < 0.001$ ). Scale bar = 5 mm. (b) BALB/c nude mice were subcutaneously inoculated with  $2 \times 10^6$  ARK2 cells (left), ARK2 wild-type and ARK2 Ser727A-mut cells (right), respectively. TBB 1 mg pretreatment (left), was administrated daily for 5 days (DMSO as a placebo), then followed with cisplatin from Day 6 (3 mg/kg BW, for 3 weeks). In addition, mice bearing ARK2 Ser727-mut cell was treated with cisplatin only from Day 6 (3 mg/kg BW, for 3 weeks). Statistical analysis was performed using two-way ANOVA analysis ( $*0.001 < p < 0.01$ ;  $***p < 0.001$ ). (c) Immunohistochemistry staining of serine-phosphorylated STAT1 expression in uterine tumors and node metastasis of patients with or without NAC containing cisplatin or carboplatin. Representative micrographs of uterine tumors and node metastasis tissues of each two patients with or without NAC were displayed, respectively. [Color figure can be viewed at [wileyonlinelibrary.com](http://wileyonlinelibrary.com)]

Fig. S4). A previous study suggested that C188-9, a STAT1 inhibitor, induces apoptosis in lung cancer cells<sup>51</sup>; however, there was no remarkable change in viability or apoptosis in USC cells treated with C188-9 (data not shown). These results indicate that it is more efficient to target STAT1 Ser727 phosphorylation to sensitize cisplatin-resistant USC than to suppress STAT1 itself. There are several kinases that can phosphorylate STAT1 at Ser727 under different cellular stresses or specific cellular environments. The p38 mitogen-activated protein kinase (p38-MAPK) pathway is generally involved in IFN-mediated Ser727 phosphorylation of STAT1 to induce apoptosis under cisplatin treatment.<sup>32</sup> Heat-shock transcription factor-1 (HSF1) and heat-shock protein 70 (HSP70) also phosphorylate STAT1 at Ser727 to enhance platinum-resistance in ovarian cancer,<sup>52</sup> HNSCC,<sup>53</sup> and Wilm's tumor.<sup>14</sup> As shown in Figure 4 and Supporting Information Figure S6, cisplatin induces Ser727 phosphorylation in two platinum-resistant USC cell lines, which was modulated by casein kinase II (CK2). As EGFR is upstream of STAT signaling, gefitinib, an EGFR inhibitor, also moderately attenuated STAT1 Ser727 phosphorylation, but its effect was not as prominent as that of the CK2 inhibitor, possibly due to other collateral signals.

CK2 is a serine/threonine phosphorylation kinase that regulates various biological processes by phosphorylating more than 200 substrates. Hence, inhibiting CK2 is an emerging strategy for cancer therapy<sup>37,52,54</sup>; specifically, CX-4945 and TBB suppress CK2 to enhance cell death caused by drugs or radiation. In our study, we first showed that STAT1 is phosphorylated at Ser727 by CK2 in USC cells in response to platinum-stress and that TBB administration prior to cisplatin treatment induces a synergistic cytotoxic effect by increasing platinum accumulation (Supporting Information Fig. S6g). As this synergistic effect was also observed in MB-MDA-231 cells, which are chemorefractory, CK2-inhibitory therapy could be used to sensitize platinum-resistant cancer cells.

TBB was not originally synthesized for clinical use. Even though low-dose administration is not overly toxic *in vitro* and *in vivo* (Supporting Information Figs. S6g and S7a), its clinical safety and efficacy remain unclear. CX-4945 (silmatasertib) is another CK2 small molecule inhibitor. Its safety was previously confirmed by a phase I clinical trial, and its clinical efficacy is currently being assessed in a phase II clinical trial.<sup>55</sup> Here, we could not use CX-4945 due to its high cost, but even CX-4945 followed by cisplatin is expected to be

effective for chemorefractory USC patients since both CX-4945 and TBB exert similar CK2 inhibiting effects.<sup>56</sup>

In summary, our study provides new insight into the treatment modality of refractory USC. The prognostic outcome for USC patients with high STAT1 expression is poor and STAT1 is involved in platinum-resistance; cisplatin-induced STAT1 Ser727 phosphorylation alters cellular platinum accumulation to promote platinum-resistance in USC, and a CK2 inhibitor suppresses STAT1 Ser727 phosphorylation to compensate for this mechanism (Fig. 6). Although it is mandatory to prospectively validate its safety and efficacy in clinical settings, scoring STAT1 status could be a biomarker to predict tumor chemoresponse, and premedication with a CK2 inhibitor could represent a potent strategy for STAT1-high USC patients to increase the efficacy of platinum-based chemotherapeutics.

### Acknowledgements

We gratefully acknowledge Dr. Santin, the Professor of Obstetrics, Gynecology and Reproductive Sciences at Yale School of Medicine for providing USC cell lines. We thank Dr. Tweardy, the Professor of Division of Internal Medicine at University of Texas MD Anderson Cancer Center for providing the STAT1 inhibitor.

### Author contributions

Experimental analysis and article writing: Zeng X, Baba T. Group supervision: Baba T and experimental design review: Matsumura N, Baba T, Abiko K and Hamanishi J. Foundational work (i.e., the previous study indicating high STAT1 expression in USC): Kharmha B. Immunohistochemistry: Mise Y. Experimental analysis conducted using the xenograft mouse model: Mulati K, Kitamura S, Taki M and Hosoe Y. Hypothesis and article writing: Hunstman DG. Article editing (department director): Mandai M.

### Ethical approval statement

Human sample studies were approved by ethics committee of Kyoto University. All human samples were acquired after written informed consent was obtained for all patients. The protocol of animal study was approved by Kyoto University Animal Research Committee.

### Data availability statement

All data generated or analyzed during this study are available from the corresponding author upon reasonable request.

### References

- Boruta DM 2nd, Gehrig PA, Fader AN, et al. Management of women with uterine papillary serous cancer: a Society of Gynecologic Oncology (SGO) review. *Gynecol Oncol* 2009;115:142–53.
- Mahdi H, Rizzo A, Rose PG. Outcome of recurrent uterine papillary serous carcinoma treated with platinum-based chemotherapy. *Int J Gynecol Cancer* 2015;25:467–73.
- Fader AN, Drake RD, O'Malley DM, et al. Uterine papillary serous carcinoma C. Platinum/taxane-based chemotherapy with or without radiation therapy favorably impacts survival outcomes in stage I uterine papillary serous carcinoma. *Cancer* 2009;115:2119–27.
- Sanchez-Vega F, Mina M, Armenia J, et al. Oncogenic signaling pathways in the cancer genome atlas. *Cell* 2018;173:321–37.e10.
- Black J, Menderes G, Bellone S, et al. SYD985, a novel Duocarmycin-based HER2-targeting antibody-drug conjugate, shows antitumor activity in uterine serous carcinoma with HER2/Neu expression. *Mol Cancer Ther* 2016;15:1900–9.
- Pennington KP, Walsh T, Lee M, et al. BRCA1, TP53, and CHEK2 germline mutations in uterine serous carcinoma. *Cancer* 2013;119:332–8.
- Kharmha B, Baba T, Matsumura N, et al. STAT1 drives tumor progression in serous papillary endometrial cancer. *Cancer Res* 2014;74:6519–30.
- Lord CJ, Ashworth A. The DNA damage response and cancer therapy. *Nature* 2012;481:287–94.

9. Martin LP, Hamilton TC, Schilder RJ. Platinum resistance: the role of DNA repair pathways. *Clin Cancer Res* 2008;14:1291–5.
10. Amable L. Cisplatin resistance and opportunities for precision medicine. *Pharmacol Res* 2016;106:27–36.
11. Zhu H, Wang Z, Xu Q, et al. Inhibition of STAT1 sensitizes renal cell carcinoma cells to radiotherapy and chemotherapy. *Cancer Biol Ther* 2012;13:401–7.
12. Varughese J, Cocco E, Bellone S, et al. Uterine serous papillary carcinomas overexpress human trophoblast-cell-surface marker (Trop-2) and are highly sensitive to immunotherapy with hRS7, a humanized anti-Trop-2 monoclonal antibody. *Cancer* 2011;117:3163–72.
13. Zhao S, Choi M, Overton JD, et al. Landscape of somatic single-nucleotide and copy-number mutations in uterine serous carcinoma. *Proc Natl Acad Sci USA* 2013;110:2916–21.
14. Timofeeva OA, Plisov S, Evseev AA, et al. Serine-phosphorylated STAT1 is a prosurvival factor in Wilms' tumor pathogenesis. *Oncogene* 2006;25:7555–64.
15. Clingen PH, Wu JY, Miller J, et al. Histone H2AX phosphorylation as a molecular pharmacological marker for DNA interstrand crosslink cancer chemotherapy. *Biochem Pharmacol* 2008;76:19–27.
16. Holohan C, Van Schaeybroeck S, Longley DB, et al. Cancer drug resistance: an evolving paradigm. *Nat Rev Cancer* 2013;13:714–26.
17. Lee PS, Fang J, Jessop L, et al. RAD51B activity and cell cycle regulation in response to DNA damage in breast cancer cell lines. *Breast Cancer (Auckl)* 2014;8:135–44.
18. Liu G, Yang D, Rupaimoole R, et al. Augmentation of response to chemotherapy by microRNA-506 through regulation of RAD51 in serous ovarian cancers. *J Natl Cancer Inst* 2015;107:djv108.
19. Lieber MR. The mechanism of double-strand DNA break repair by the nonhomologous DNA end-joining pathway. *Annu Rev Biochem* 2010;79:181–211.
20. Chirnomas D, Taniguchi T, de la Vega M, et al. Chemosensitization to cisplatin by inhibitors of the Fanconi anemia/BRCA pathway. *Mol Cancer Ther* 2006;5:952–61.
21. Samimi G, Fink D, Varki NM, et al. Analysis of MLH1 and MSH2 expression in ovarian cancer before and after platinum drug-based chemotherapy. *Clin Cancer Res* 2000;6:1415–21.
22. McNeil EM, Melton DW. DNA repair endonuclease ERCC1-XPF as a novel therapeutic target to overcome chemoresistance in cancer therapy. *Nucleic Acids Res* 2012;40:9990–10004.
23. Choi DW, Na W, Kabir MH, et al. WIP1, a homeostatic regulator of the DNA damage response, is targeted by HIPK2 for phosphorylation and degradation. *Mol Cell* 2013;51:374–85.
24. Wang X, Jiang P, Wang P, et al. EGCG enhances cisplatin sensitivity by regulating expression of the copper and cisplatin influx transporter CTR1 in ovary cancer. *PLoS One* 2015;10:e0125402.
25. Liang ZD, Long Y, Tsai WB, et al. Mechanistic basis for overcoming platinum resistance using copper chelating agents. *Mol Cancer Ther* 2012;11:2483–94.
26. Larson CA, Adams PL, Jandial DD, et al. The role of the N-terminus of mammalian copper transporter 1 in the cellular accumulation of cisplatin. *Biochem Pharmacol* 2010;80:448–54.
27. Komatsu M, Sumizawa T, Mutoh M, et al. Copper-transporting P-type adenosine triphosphatase (ATP7B) is associated with cisplatin resistance. *Cancer Res* 2000;60:1312–6.
28. Surowiak P, Materna V, Maciejczyk A, et al. Nuclear metallothionein expression correlates with cisplatin resistance of ovarian cancer cells and poor clinical outcome. *Virchows Arch* 2007;450:279–85.
29. Redell MS, Ruiz MJ, Alonzo TA, et al. Stat3 signaling in acute myeloid leukemia: ligand-dependent and -independent activation and induction of apoptosis by a novel small-molecule Stat3 inhibitor. *Blood* 2011;117:5701–9.
30. Kovarik P, Mangold M, Ramsauer K, et al. Specificity of signaling by STAT1 depends on SH2 and C-terminal domains that regulate Ser727 phosphorylation, differentially affecting specific target gene expression. *EMBO J* 2001;20:91–100.
31. Thomas M, Finnegan CE, Rogers KM, et al. STAT1: a modulator of chemotherapy-induced apoptosis. *Cancer Res* 2004;64:8357–64.
32. Ramsauer K, Sadzak I, Porras A, et al. p38 MAPK enhances STAT1-dependent transcription independently of Ser-727 phosphorylation. *Proc Natl Acad Sci USA* 2002;99:12859–64.
33. Gartsbein M, Alt A, Hashimoto K, et al. The role of protein kinase C delta activation and STAT3 Ser727 phosphorylation in insulin-induced keratinocyte proliferation. *J Cell Sci* 2006;119:470–81.
34. Li N, McLaren JE, Michael DR, et al. ERK is integral to the IFN-gamma-mediated activation of STAT1, the expression of key genes implicated in atherosclerosis, and the uptake of modified lipoproteins by human macrophages. *J Immunol* 2010;185:3041–8.
35. Nguyen H, Ramana CV, Bayes J, et al. Roles of phosphatidylinositol 3-kinase in interferon-gamma-dependent phosphorylation of STAT1 on serine 727 and activation of gene expression. *J Biol Chem* 2001;276:33361–8.
36. Nair JS, DaFonseca CJ, Tjernberg A, et al. Requirement of Ca<sup>2+</sup> and CaMKII for Stat1 Ser-727 phosphorylation in response to IFN-gamma. *Proc Natl Acad Sci USA* 2002;99:5971–6.
37. Siddiqui-Jain A, Bliesath J, Macalino D, et al. CK2 inhibitor CX-4945 suppresses DNA repair response triggered by DNA-targeted anticancer drugs and augments efficacy: mechanistic rationale for drug combination therapy. *Mol Cancer Ther* 2012;11:994–1005.
38. So KS, Rho JK, Choi YJ, et al. AKT/mTOR down-regulation by CX-4945, a CK2 inhibitor, promotes apoptosis in chemorefractory non-small cell lung cancer cells. *Anticancer Res* 2015;35:1537–42.
39. Fritz G, Issinger OG, Olsen BB. Selectivity analysis of protein kinase CK2 inhibitors DMAT, TBB and resorufin in cisplatin-induced stress responses. *Int J Oncol* 2009;35:1151–7.
40. Chou TC. Drug combination studies and their synergy quantification using the Chou-Talalay method. *Cancer Res* 2010;70:440–6.
41. Kovacic B, Stoiber D, Moriggl R, et al. STAT1 acts as a tumor promoter for leukemia development. *Cancer Cell* 2006;10:77–87.
42. Khodarev NN, Minn AJ, Efimova EV, et al. Signal transducer and activator of transcription 1 regulates both cytotoxic and prosurvival functions in tumor cells. *Cancer Res* 2007;67:9214–20.
43. Federico MB, Vallergera MB, Radl A, et al. Chromosomal integrity after UV irradiation requires FANCD2-mediated repair of double strand breaks. *PLoS Genet* 2016;12:e1005792.
44. Wu X, Fan W, Xu S, et al. Sensitization to the cytotoxicity of cisplatin by transfection with nucleotide excision repair gene xeroderma pigmentosum group A antisense RNA in human lung adenocarcinoma cells. *Clin Cancer Res* 2003;9:5874–9.
45. Selvakumaran M, Pisarcik DA, Bao R, et al. Enhanced cisplatin cytotoxicity by disturbing the nucleotide excision repair pathway in ovarian cancer cell lines. *Cancer Res* 2003;63:1311–6.
46. Konstantinopoulos PA, Ceccaldi R, Shapiro GI, et al. Homologous recombination deficiency: exploiting the fundamental vulnerability of ovarian cancer. *Cancer Discov* 2015;5:1137–54.
47. Jones NL, Xiu J, Reddy SK, et al. Identification of potential therapeutic targets by molecular profiling of 628 cases of uterine serous carcinoma. *Gynecol Oncol* 2015;138:620–6.
48. Yoshizawa K, Nozaki S, Kitahara H, et al. Copper efflux transporter (ATP7B) contributes to the acquisition of cisplatin-resistance in human oral squamous cell lines. *Oncol Rep* 2007;18:987–91.
49. Surowiak P, Materna V, Kaplenko I, et al. Augmented expression of metallothionein and glutathione S-transferase pi as unfavourable prognostic factors in cisplatin-treated ovarian cancer patients. *Virchows Arch* 2005;447:626–33.
50. Wang J, Wu GS. Role of autophagy in cisplatin resistance in ovarian cancer cells. *J Biol Chem* 2014;289:17163–73.
51. Xu X, Kasembeli MM, Jiang X, et al. Chemical probes that competitively and selectively inhibit Stat3 activation. *PLoS One* 2009;4:e4783.
52. Kao C, Chao A, Tsai CL, et al. Phosphorylation of signal transducer and activator of transcription 1 reduces bortezomib-mediated apoptosis in cancer cells. *Cell Death Dis* 2013;4:e512.
53. Schmitt NC, Trivedi S, Ferris RL. STAT1 activation is enhanced by Cisplatin and variably affected by EGFR inhibition in HNSCC cells. *Mol Cancer Ther* 2015;14:2103–11.
54. Yang B, Yao J, Li B, et al. Inhibition of protein kinase CK2 sensitizes non-small cell lung cancer cells to cisplatin via upregulation of PML. *Mol Cell Biochem* 2017;436:87–97.
55. Chon HJ, Bae KJ, Lee Y, et al. The casein kinase 2 inhibitor, CX-4945, as an anti-cancer drug in treatment of human hematological malignancies. *Front Pharmacol* 2015;6:70.
56. Gray GK, McFarland BC, Rowse AL, et al. Therapeutic CK2 inhibition attenuates diverse prosurvival signaling cascades and decreases cell viability in human breast cancer cells. *Oncotarget* 2014;5:6484–96.